minerals

MDPI

Article

Characterization of Tableware from Fábrica de Loiça de Sacavém—Linking Analytical and Documental Research

Mathilda L. Coutinho [1,*], João Pedro Veiga [2,3,4], Andreia Ruivo [3,4], Teresa Pereira da Silva [5], Silvia Bottura-Scardina [1], Maria Margarida R. A. Lima [2,6], Carlos Pereira [7], Ana Carvalho Dias [8], Luis Dias [1], Peter Vandenabeele [9,10] and José C. Roseiro [11]

1 HERCULES Laboratory—City University of Macau Chair in Sustainable Heritage—Institute for Advanced Studies and Research, Laboratório Associado IN2PAST, University of Évora, 7000-809 Évora, Portugal; scardina@uevora.pt (S.B.-S.); luisdias@uevora.pt (L.D.)
2 CENIMAT/I3N, Centro de Investigação de Materiais, Faculdade de Ciências e Tecnologia, Universidade NOVA de Lisboa, Quinta da Torre, 2829-516 Caparica, Portugal; jpv@fct.unl.pt (J.P.V.); mmal@fct.unl.pt (M.M.R.A.L.)
3 Departamento de Conservação e Restauro, Faculdade de Ciências e Tecnologia, Universidade NOVA de Lisboa, Quinta da Torre, 2829-516 Caparica, Portugal; a.ruivo@fct.unl.pt
4 VICARTE, Research Unit Vidro e Cerâmica para as Artes, Faculdade de Ciências e Tecnologia, Universidade NOVA de Lisboa, 2829-516 Caparica, Portugal
5 Unidade de Recursos Minerais e Geofísica, Laboratório Nacional de Energia e Geologia, 2610-999 Amadora, Portugal; teresa.pena@lneg.pt
6 Departamento de Ciência dos Materiais, Faculdade de Ciências e Tecnologia, Universidade NOVA de Lisboa, Quinta da Torre, 2829-516 Caparica, Portugal
7 Museu da Cerâmica de Sacavém, Câmara Municipal de Loures, Praça Manuel Joaquim Afonso, 2685-145 Sacavém, Portugal
8 Direção-Geral do Património Cultural (DGPC), Largo da Ajuda, 1349-021 Lisbon, Portugal; anamosacdias@gmail.com
9 Raman Spectroscopy Research Group, Department of Chemistry, Ghent University, Ghent, Krijgslaan 281, B-9000 Ghent, Belgium; peter.vandenabeele@ugent.be
10 Archaeometry Research Group, Department of Archaeology, Ghent University, Sint-Pietersnieuwstraat 35, B-9000 Ghent, Belgium
11 Associação dos Amigos da Loiça de Sacavém, Rua dos Milagres, nº 4, Folgorosa, Dois Portos, 2765-171 Torres Vedras, Portugal; jose.roseiro@lneg.pt
* Correspondence: magldc@uevora.pt or mathildal@gmail.com

Abstract: Fábrica de Loiça de Sacavém (ca. 1858–1994) was among the first to produce white earthenware in Portugal, becoming one of the country's leading ceramic manufacturers during the late 19th to early 20th centuries. Research on white earthenware has accompanied the growing interest in post-industrial archaeology but is still poorly explored compared to more ancient ceramic productions. This study focused on the ceramic body, glazes, and colourants of tableware produced by Fábrica de Loiça de Sacavém during the first 50 years of its activity (1859–1910). A multi-analytical approach was selected to investigate the chemical and mineralogical composition of the ceramic body, glaze, and pigments using optical microscopy, variable-pressure scanning electron microscope energy-dispersive X-ray spectroscopy (VP-SEM-EDS), μ-Raman spectroscopy, μ-X-ray Diffraction (μ-XRD), and reflectance spectroscopy (hyperspectral image analysis). The studied tableware was produced with a Ca-poor siliceous–aluminous white earthenware ceramic body covered with transparent alkali lead or lead borosilicate glaze, and most colourants were complex Cr-based pigments. These results are in agreement with the little documental evidence from this period found in the manufacturer's archives.

Keywords: glazes; ceramic pigments; white industrial earthenware; SEM; Raman

Citation: Coutinho, M.L.; Veiga, J.P.; Ruivo, A.; Pereira da Silva, T.; Bottura-Scardina, S.; Lima, M.M.R.A.; Pereira, C.; Dias, A.C.; Dias, L.; Vandenabeele, P.; et al. Characterization of Tableware from Fábrica de Loiça de Sacavém—Linking Analytical and Documental Research. *Minerals* **2024**, *14*, 324. https://doi.org/10.3390/min14030324

Academic Editor: Domenico Miriello

Received: 6 January 2024
Revised: 2 March 2024
Accepted: 15 March 2024
Published: 21 March 2024

1. Introduction

During the 19th century, white earthenware became a massive success due to its similarity to porcelain at a more affordable price. This specific ceramic class is characterised by a white and porous ceramic body, which began to be produced during the mid-18th century [1–4]. The exact origin of its invention is still controversial since it appears almost simultaneously in England and France [1,2,4]. The production of white earthenware accompanied a fast technological evolution due to consumers' increasing demands. Variations in the recipes for aesthetic and mechanical improvements included adding calcined flint to the ceramic body, using kaolin and feldspar to increase hardness, or using cobalt to whiten the ceramic body by optically masking its yellow hue [5]. Maggetti [5] describes two main families of white earthenware ceramic pastes: CaO-poor and CaO-rich. The CaO-poor ceramic bodies were obtained from Ca-poor clays mixed with silica aggregates (e.g., calcined flint, quartz, pebbles or sand) and fluxes (e.g., illite, Cornish stone, or grog) [5]. In turn, Ca-rich ceramic bodies were produced directly from calcium-rich clays or by adding calcium carbonates to CaO-poor clays [3,5]. Calcium affects the volume variation and the type of mineral phases formed during the firing, depending on the composition of the ceramic body and sintering process [6]. Ca-rich earthenware are usually fired at lower temperatures, being less hard then Ca-poor earthenware, which can be fired at higher temperatures [7]. In summary, the multiple recipes used by manufacturers during this period resulted in ceramic bodies with distinctive chemical compositions and micromorphological features, and this enables distinctions between manufacturers to be studied [2–4,8].

Most earthenware manufacturers applied transparent lead alkali or lead borosilicate glazes, and only a few exceptions used tin-opacified glaze [3,8,9]. The glaze recipes also seem to have suffered alterations, mainly to increase mechanical resistance [9]. English manufacturers mostly used transfer print technology to decorate their ceramic products [10]. This involved applying ceramic pigments or metal oxides mixed with boiled linseed oil and powdered flint onto a copper plate with an engraved design, which was then transferred through tissue paper or a glue bat (gelatine sheet) to the ceramic object [3,10]. The available colour palette also changed significantly during the 19th century due to the development of many chromium-based pigments [11].

In Portugal, white industrial earthenware technology only arrived in the mid-19th century, *Fábrica de Loiça de Sacavém* (ca. 1858–1994) ("Sacavém ceramic manufacture"—FLS herein after) was a pioneer in introducing, implementing, and disseminating white earthenware in the country [12–14]. In Portugal, the tableware industry was firmly rooted in redware or earthenware coated with tin-opacified glazes [12–14]. The history of the FLS manufactory can be summarised according to its successive ownerships, administrators, or accomplishments [15]; (i) Manuel Joaquim Afonso (MJA) was the founder of the manufactory during the last years of 1850s [15]; (ii) In the second period, a British family—the Stott Howorth family—started exploring FLS and introduced novel technology imported directly from England. First, the factory was leased to William John Howorth (1821–1905), and later, his brother John Stott Howorth (1829–1893) took over in 1972 after a financial crisis; (iii) In 1885, King Dom Luís awarded J. S. Howorth the title *Barão* (Baron) *Howorth de Sacavém*, and the factory was given the privilege of being entitled *Real* (Royal) *Fábrica de Sacavém* (hereinafter RFS); (iv) In 1893, the widow of J. S. Howorth inherited the factory after his death, and the bookkeeper James Gilman was assigned as representative, being given full authority to conduct and manage the factory. The following year, both formed the Baronesa de Howorth de Sacavém & Companhia; (v) Herbert Gilbert joined the company in 1907, also as a bookkeeper, and later become a business partner and shareholder; (vi) In the 1930s, the Gilbert family began to take a leading role in the administration of FLS. The factory's production lasted until 1994. Following its definitive closure, a museum—*Museu de Cerâmica de Sacavém* (MCS)—was built surrounding the structure of one of the factory's kilns where a significant collection of objects is now in display. Also, an archive—*Centro de Documentação Manuel Joaquim Afonso*—has many documents related to the factory's

production; however, little documental evidence has survived from the first 50 years of labour.

Recently, English, French, and Swiss manufacturers of white earthenware, dating from the 18th to the 20th centuries, have investigated material and technological production [1,3–5,9]. Still, few articles have studied the colourants produced during this period [16]. Numerous studies have focused on the historical, cultural, and archival aspects of Sacavém's production [15,17–19]. However, no study has focused on the technological and material aspects of tableware production. The material studies of the early production of FLS, as a pioneer in the production of white industrial earthenware, is essential to understanding the technological advancements in the Portuguese ceramic industry, such as the development of novel ceramic bodies and glazes and the introduction of colourants. Tableware objects with representative colours, covering the main production periods of 50 years of production (ca. 1859 to 1910)—MJA, FLS, and RFS—were analysed in this study. SEM-EDS and m-XRD were applied to characterise the ceramic body to determine elemental and mineralogical composition. The composition of the glaze and pigments was studied concerning production technology, using scanning electron microscope energy-dispersive X-ray spectroscopy (SEM-EDS), X-ray diffraction, reflectance spectroscopy (his), and μ-Raman.

2. Materials and Methods

2.1. Materials

This study focuses on a set of 17 tableware objects dated from the first fifty years of production (1859–1910). The objects were provided by the Museu de Cerâmica de Sacavém (MCS) (Loures, Portugal), by the Associação dos Amigos da Loiça de Sacavém (AALS), and archaeological shards excavated in Convento de Cristo (Arq_CC) (Table 1 and Figure 1). The archaeological shards were unearthed from a nitre pit in Convento de Cristo in 2015, being an important testimony of the daily life of the convent after the extinction of the religious orders in Portugal.

Table 1. List with details of the analysed tableware from the Sacavém Ceramic Factory (Portugal) (reference or catalogue number, typology, provenance, colour, period, and name of the decoration motif).

Ref.	Typology	Provenance [1]	Colour	Period	Motif
SAC1	Plate	AALS	Strong blue	RFS-G	TOGG
SAC2	soup plate	AALS	Black	FS	Statue
SAC4	soup plate	AALS	Light blue	RFS	Ornato
SAC7	plate	AALS	Green	RFS	Pheasant
SAC12	plate	AALS	Green	RFS	Pheasant
SAC13	soup plate	AALS	Brown	FS	Metz
SAC14	plate	AALS	Blue lavender	RFS	Statue
SAC16	plate	AALS	Blue lavender	FS	Venice
SAC18	plate	AALS	Blue lavender	FS	Venice
CC_NEC_5	plate	Arq_CC	Green	FS	Statue
CC_NEC_14	plate	Arq_CC	Green	RFS	Statue
CC_NEC_16	plate	Arq_CC	Green	RFS	Statue
CC_NEC_59	plate	Arq_CC	Strong blue	FS	Statue
CC_NEC_110	plate	Arq_CC	Black	RFS	Statue
MCS1	dish	MCS	Light blue	MJA	-
MCS14	dish	MCS	Brown	FS	Oriental
MCS 9358	plate	MCS	Pink	RFS	Willow

[1] AALS—Associação dos Amigos da Loiça de Sacavém; Arq_CC—archaeological context from the Convento de Cristo (Tomar, Portugal); MCS—Museu de Cerâmica de Sacavém.

Figure 1. Examples of the main colours produced by the ceramic manufacturer FLS: blue (SAC1), black (SAC2), green (SAC12), brown (SAC13), lavender (SAC16), and pink (MCS9358).

The objects were classified into four groups: Manuel Joaquim Afonso (MJA); *Fábrica de Loiça de Sacavém* (FLS), produced before 1885; *Real Fábrica de Sacavém* (RFS), produced between 1885 and 1910; and *Real Fábrica de Sacavém* Granito (RFS-G).

The set of 17 objects with previous damages were sampled with plyers. Cross-sections were prepared by mounting the samples in EpoFix® resin (Struers ApS, Ballerup, Denmark). Subsequently, the resin blocks were dried for at least 24 h and polished with a RotoPol-35® instrument (Struers, Denmark), then cleaned with an ultrasound bath for 10 min and dried for 24 h.

2.2. Manuscript from the Archive of Fábrica de Loiça de Sacavém

A manuscript (*Pasta nº4, Centro de Documentação Manuel Joaquim Afonso*) of an unknown author, which could be described as an arcanum, comprises several recipes (ceramic bodies, glazes, and ceramic colours), technical notes, references to suppliers of raw materials, and even copies of letters. This document has no precise date, although it must be dated from the late 19th or early 20th century, since it was written on an English almanac of the year 1881 and has a copy of a letter to Mr. Gilman in which invoices dating from May 1906 are present. Its recipes, which seem to have been collected from different ceramic manufacturers in England, were compared with the results obtained through the analytical approach.

2.3. Analytical Approach

2.3.1. X-ray Microdiffraction (Micro-XRD)

XRD was performed in order to identify crystalline phases of the ceramic body with a Da Vinci AXS D8 Discover (Bruker, Germany) with a Cu Kα source, operating at 40 kV and 40 mA, and a Lynxeye1-dimensional detector. Scans were collected from 3 to 75° 2θ, with 0.05 2θ step and 1 s/step measuring time by point. Phase Diffract-Eva software with a PDF-2 mineralogical database was utilised for phase analysis and identification. The collected samples were analysed before mounting in resin.

2.3.2. Vis-SWIR Reflectance Spectroscopy

A set of 6 ceramic objects with different colours was analysed by Vis-SWIR (Visible-Short Wave infrared) imaging with a Specim IQ mobile hyperspectral camera (Specim Ltd., Oulu, Finland) to acquire hypercubes. A Si-CMOS sensor collects data in the spectral region ranging from 400 to 1000 nm in 204 bands with a spectral resolution of 7 nm to generate 512 × 512 element data. The equipment automatically performs background correction, and all assays were recorded with a white reference panel (Specim Ltd.) for colour calibration with the built-in software for in situ data acquisition and validation. For the illumination, a halogen lamp (1000 W, temperature colour 3200 K) was placed at ca. 1 m distance from the samples. Halogen lamps were used with a photo light reflector being positioned to draw a 40° light incidence angle, ensuring diffuse illumination of the object and preventing specular reflectance. Three representative reflectance spectra were extracted for each sample from the acquired hypercubes using the ENVI analysis software (ENVI Classic 5.3, Exelis VIS, Boulder, CO, USA), being subjected to the Kubelka–Munk model.

2.3.3. Optical Microscope (OM)

Magnified cross-section images were acquired under a Leica M205C stereoscope (Leica Microsystems GmbH, Wetzlar, Germany) with a zoom range of 7.8× to 160× equipped with a Leica DFC295 camera and an external racking illumination by optical fibres.

2.3.4. Variable-Pressure Scanning Electron Microscopy—Energy-Dispersive X-ray Spectroscopy (VP-SEM-EDS)

A set of 11 cross-sections were examined on a Hitachi 3700 N scanning electron microscope (Hitachi, Tokyo, Japan) interfaced with a Quantax EDS microanalysis system (Bruker AXS GmbH, Karlsruhe, Germany). The Quantax system was equipped with a Bruker AXS XFlash Silicon Drift Detector (129 eV spectral resolution at full width at half maximum [FWHM]—Mn Ka). The operating conditions were 40 Pa, 20 kV accelerating voltage, 10 mm working distance, and 75 μA emission current. The data were collected and processed using the software Esprit 1.9. Only major and minor elements were quantified and converted into oxides (Na_2O, MgO, Al_2O_3, SiO_2, K_2O, CaO, TiO_2, Fe_2O_3, and PbO). Standard glass CMOG C was analysed, and the measured values of the studied elements are presented in Table S1. No surface coating was applied to allow for other analysis.

2.3.5. Field Emission Scanning Electron Microscopy—Energy-Dispersive X-ray Spectroscopy (FE-SEM-EDS)

Three cross sections, MCS1, MCS14 and MCS9358, were analysed to investigate the formation of mullite in the ceramic body via Field Emission Scanning Electron Microscopy (TESCAN Clara, Kohoutovice, Czech Republic), using 15kV accelerating voltage and 10 mm working distance and 100 Pa chamber pressure. The micrographs were obtained with a backscattered electron detector (LE-BSE). The EDS experiments were performed with an X-ray spectrometer Bruker XFlash 6130 SDD detector with 126 eV spectral resolution at the FWHM/Mn Kα, coupled to the previous instrument and using the same conditions. The data were collected and processed using the software Esprit 2.5.

2.3.6. Micro-Raman Spectroscopy (μ-Raman)

Mineralogical characterisation of the mineral inclusions of the glaze and pigments was carried out directly on the cross-sections using a Labram 300 Jobin–Yvon spectrometer (Horiba Scientific, Paris, France), equipped with an external solid-state laser with 50 mW power, operating at 514.5 nm. Spectra were recorded as extended scans, and the laser beam was focused either with a 50× or 100× Olympus objective lens. The laser power at the samples' surface was varied with a set of neutral density filters (optical densities 0.3, 0.6, 1, and 2).

3. Results and Discussion

3.1. Ceramic Body

The main mineral phases identified in the diffractograms of the ceramic body were quartz, cristobalite, and mullite (Figure 2). Both cristobalite and mullite are neoformation phases resulting from the transformations of other mineral phases during firing. Depending on the ceramic paste's raw materials and composition, these mineral phases can be formed above 1000 or 1050 °C [20]. Mullite is a non-stoichiometric compound with a composition between $3Al_2O_3$-$2SiO_2$ and $2Al_2O_3$-SiO_2 that can be obtained by the thermal decomposition of kaolinite, and cristobalite [21] is a crystalline form of silica formed in the matrix of clay bodies. The studied samples showed variations in the ratio of cristobalite and mullite. The ceramic body of MJA presents a very high cristobalite peak (Figure 2—MCS 1), FLS and RFS presented peaks in two situations—similar intensity or weak cristobalite peak, and RSFS-G presented a very weak cristobalite peak. The decrease in cristobalite may be related to lower firing temperature or changes in the raw materials (type of clay) [20]. CaO-poor whitewares from Creil, Pont-aux-Choux, Sarreguemines, and Wedgwood [5] showed crystalline phases similar to those of the Sacavém factory. According to the same study, this would indicate firing temperatures above 1050 °C, corroborating previous studies that estimated that this ceramic body type would have been fired at temperatures of 1200–1250 °C.

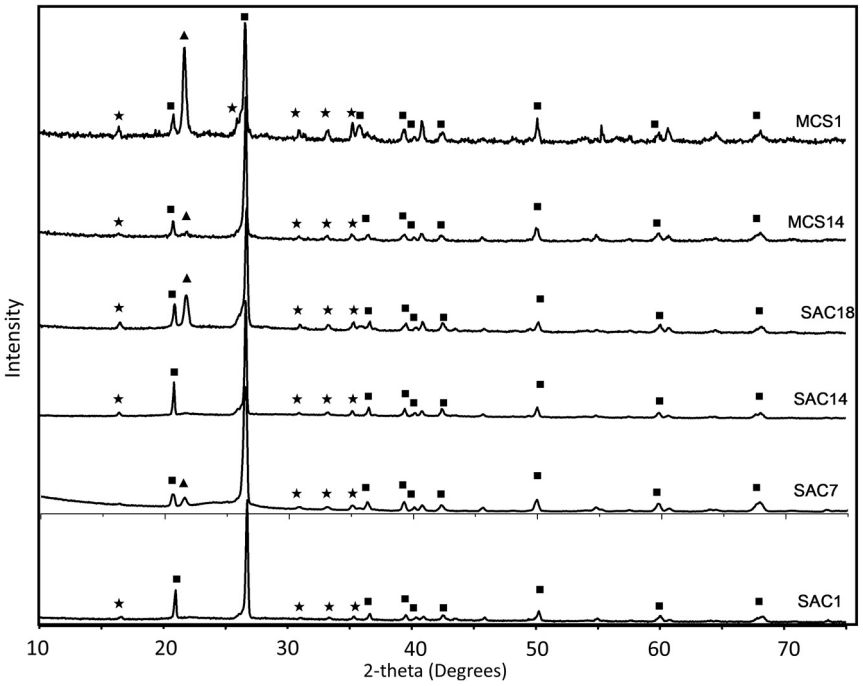

Figure 2. Diffractograms of the ceramic bodies of tableware from the Sacavém factory. Quartz—square; Mullite—star; Cristobalite—triangle.

Observation of the ceramic body cross-sections under VP-SEM showed a microstructure with abundant Si-rich particles dispersed within a porous fine-grained siliceous–aluminous matrix assembled with interparticle glass (Figure 3).

The microstructure also denotes some variations during the studied period (Figure 3), particularly regarding the morphology of the Si-rich particles (size and shape) and the degree of vitrification. MJA (MCS1) showed a combination of coarser heterogeneously shaped SiO_2 particles and small grains (Figure 3—MCS1). The FLS objects evidenced that some technological changes might have occurred during this period. While some samples had a microstructure similar to the MJA-sample (Figure 3—SAC16), others had smaller, more angular-shaped SiO_2 grains. The RFS-marked objects were more vitrified and had more heterogenous SiO_2 particles. In the granite-type ceramic bodies (RFS-

G), the Si grains had rounded edges (Figure 4—RFS-G). The ceramic bodies had two typologies of Si-rich grains, both identified as quartz. In most of the studied samples, the Si-rich grains had internal cracks and micrometric porosity (Figure 4). These features are characteristic of calcined flint [5], which is a hard rock composed of cryptocrystalline quartz or amorphous silica [22]. Calcined flint is easier to grind and becomes whiter due to thermal treatment [23]. Also, the calcination removes water from hydrated phases, oxidises carbonaceous matter, and ensures that all amorphous silica (e.g., opal) is transformed into quartz [23]. On the contrary, SAC1 presented dense Si-particles (Figure 3 SAC1) related to macrocrystalline forms of quartz obtained, such as quartz rock, sand, or sandrock [22]. Adding cryptocrystalline quartz or macrocrystalline quartz affects the final properties of ceramics products. For instance, flint is more easily converted into cristobalite than other coarser-grained varieties of silica [22]. This fact could explain the variation in the cristobalite peak in the XRD results. Regarding documental evidence, Charles Lepierre [12,13] performed a chemical analysis of production in the Sacavém factory during the final decades of the 19th century in the book *Estudo Chimico e Tecnológico da Cerâmica Portuguesa Moderna* (Chimical and Technological Study of the Portuguese Modern Ceramics), first published in 1899. According to this reference, the Sacavém factory added flint ("seixos") to the ceramic paste recipe [12,13].

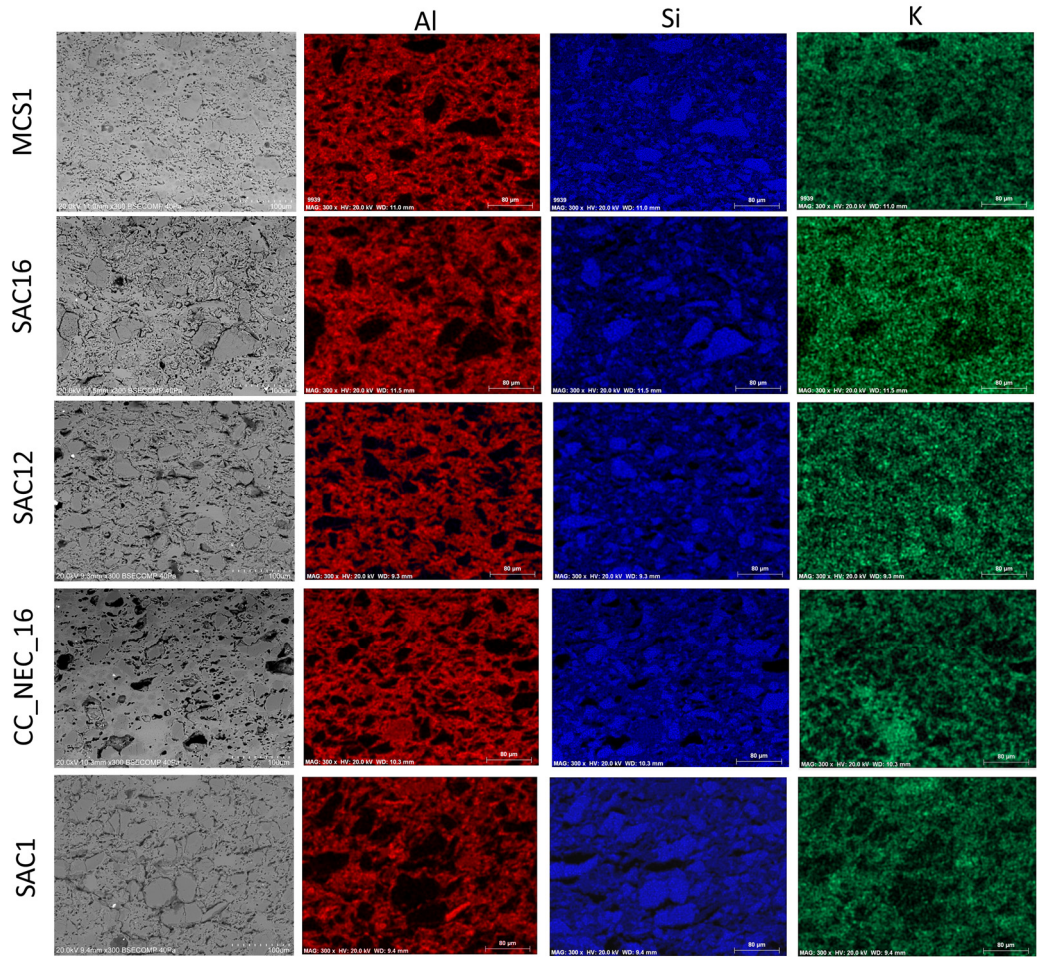

Figure 3. Backscattering scanning electron microscope (SEM-BSE) images and elemental maps of Al, Si, and K of the ceramic bodies marked with five different stamps from Fábrica de Sacavém. MCS 1, example of MJA; SAC 16, example of FLS; SAC 2, example of RFS; SAC 12, example of RFS; CC_NEC_16, example of RFS; and SAC 1, example of RFS-granite.

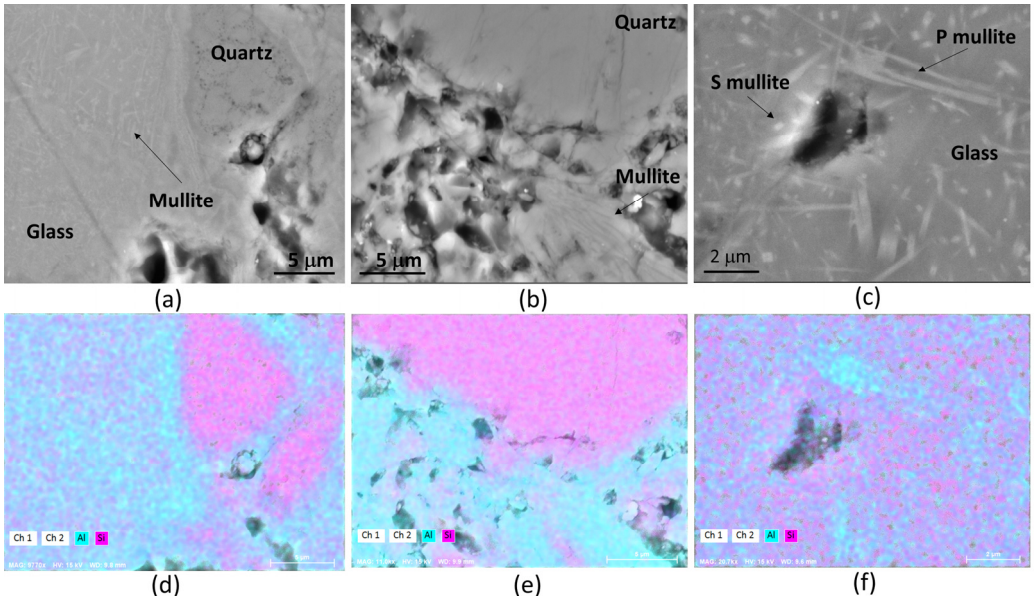

Figure 4. Backscattering scanning electron microscope (FE-SEM) images of the ceramic bodies (identified as quartz, glass, and mullite crystals) and corresponding Si and Al elemental maps of samples MCS1 (**a**,**d**), MCS14 (**b**,**e**), and MCS9358 (**c**,**f**).

To observe the Al-Si-rich phase of the ceramic body, some samples were observed under FE-SEM. The network that forms the porous body seems to be formed of a glassy phase with a precipitation of Al-rich crystals. These are related to primary and secondary mullite crystals formed within a vitreous part. At higher magnifications, their typical morphological features [24] could be observed, with the primary mullite showing long needle-shaped crystals and the secondary mullite presenting smaller crystals (Figure 4c,f).

Adding glass or minerals that form vitreous phases, such as feldspar or Cornwall stone, was used to reduce the porosity and ensure the inter-grain glass that holds the ceramic body together (Figure 4). The samples produced during the RFS seem to present particles richer in K, which could indicate the addition of K-rich mineral sources such as Cornish stone or feldspar.

The composition of all studied ceramic bodies had SiO_2 and Al_2O_3 as the main components within a range between ca. 15–27 wt.% and 63–77 wt.%, respectively (Table S1). This chemical composition falls within the siliceous–aluminous white earthenware ceramics [1]. The content of K_2O was low, ranging between 1 and 3 wt.%. All other detected elements, Na_2O, MgO, CaO, TiO_2, and Fe_2O_3, were below two wt.%. The chemical composition of all studied types—MJA, FLS, RFS, and RFS-G—were very similar. According to Lepierre, the ceramic body of FLS was composed of 72.1 wt.% of SiO_2, 24.0 wt.% of Al_2O_3, 0.7 wt.% of Fe_2O_3, 1.8 wt.% of CaO, 0.8 of MgO, and 0.3 wt.% of alkalis and other undetermined elements [12,13]. The results obtained for all the samples resemble the composition mentioned by Lepierre.

3.2. Transparent Glaze

The transparent glazes were mainly composed of SiO_2, Al_2O_3, and PbO, with values ranging between 51–65 wt.%, 12–17 wt.%, and 5 –19 wt.%, respectively. CaO was also present in high concentrations of ca. 4.5–9wt.% (Table 2). Samples from FLS and G-RFS presented lower concentrations (4.6–6.8 wt.%) than the RFS (8.1–9.1 wt.%) (Table 2). The alkalis content of Na_2O and K_2O ranged from 1.3 to 3.6 wt.% and 2.6 to 4.25 wt.%, respectively. Other oxides, such as MgO, TiO_2, and Fe_2O_3, were detected in percentages below one. In some of the samples, Co, Zn, P, and Ba were also detected. Co and Zn may be associated with colourants.

Table 2. Composition (max.–min.) in oxides (wt.%) of the transparent glaze measured via EDS analysis.

Period	Sample		Na_2O	MgO	Al_2O_3	SiO_2	K_2O	CaO	TiO_2	Fe_2O_3	CoO	ZnO	BaO	PbO
MJA	MCS1	σ	3.7	0.1	13.7	51.2	3.5	9.5	0.1	0.6	n.d.	n.d.	n.d.	19.3
		S.D.	0.1	0.1	0.4	1.0	0.1	0.1	0.04	0.05	-	-	-	0.5
FLS	SAC2	σ	3.7	0.5	17.1	64.4	3.7	4.5	0.2	0.9	0.4	n.d.	0.03	4.6
		S.D.	0.1	0.1	0.8	1.7	0.2	0.6	0.0	0.3	0.1	-	0.02	0.5
	SAC13	σ	2.1	0.2	14.3	59.3	3.4	5.1	0.2	0.5	n.d	n.d	0.8	14.2
		S.D.	0.2	0.1	1.3	0.4	0.5	1.0	0.0	0.2	-	-	0.1	1.2
	SAC16	σ	1.9	0.3	13.9	60.5	3.5	6.6	0.1	0.5	n.d	n.d	1.1	11.5
		S.D.	0.1	0.03	0.3	1.9	0.2	0.3	0.03	0.1	-	-	0.2	1.0
	CC_NEC_59	σ	1.4	0.2	14.2	58.6	3.4	5.7	0.3	0.4	0.2	n.d	0.8	14.7
		S.D.	0.1	0.02	0.7	0.8	0.3	0.5	0.4	0.1	0.1	-	0.6	0.5
	CC_NEC_5	σ	1.3	0.2	12.2	58.3	3.3	6.8	0.1	0.5	n.d.	n.d	1.2	16.1
		S.D.	0.1	0.0	0.3	0.7	0.0	0.1	0.0	0.0	-	-	0.1	0.7
RFS	CC_NEC_14	σ	2.5	0.1	13.3	55.0	3.1	9.4	0.2	0.7	0.4	2.9	n.d.	12.4
		S.D.	0.2	0.1	0.5	1.4	0.1	0.8	0.03	0.2	0.1	0.3	-	0.9
	SAC14	σ	2.0	0.2	15.8	58.7	4.3	9.5	0.1	0.6	n.d.	n.d.	n.d.	8.8
		S.D.	0.1	0.5	0.6	1.3	0.1	0.1	0.04	0.1	-	-	-	0.9
	SAC12	σ	1.7	0.2	15.4	60.2	4.0	8.9	0.2	0.5	n.d.	n.d.	n.d.	8.9
		S.D.	0.1	0.0	0.5	1.3	0.1	0.3	0.0	0.1	-	-	-	0.6
	MCS9358	σ	2.3	0.2	16.1	58.6	3.7	8.7	0.2	0.6	0.03	n.d.	n.d.	9.5
		S.D.	0.2	0.0	0.1	0.8	0.2	0.9	0.0	0.1	0.04	-		0.5
RFS-G	SAC1	σ	1.6	0.2	14.7	65.2	4.8	5.6	0.2	0.4	n.d.	n.d.	0.1	7.2
		S.D.	0.1	0.0	0.3	0.6	0.1	0.2	0.1	0.0	-	-	0.1	0.2
CMOGC	Measured	σ	3.7	0.5	17.1	64.4	3.7	4.5	0.2	0.9	n.d.	n.d.	11.8	36.8
		S.D.	0.1	0.1	0.8	1.7	0.2	0.6	0.0	0.3	-	-	0.1	3.9
	Ref.		2.1	0.2	14.3	59.3	3.4	5.1	0.2	0.5	0.18	0.052	11.4	36.7

The analysis of the ratio of SiO_2 and PbO in the glazes showed a distinction between the FLS, RFS, and G-RFS samples (Figure 5). Only sample SAC 2 showed some surprising results, with a much lower Pb ration. The results suggest that MJA (MCS1) had a higher amount of lead that decreased through time, being the G-RFS recipes of (SAC1) the one presenting less lead.

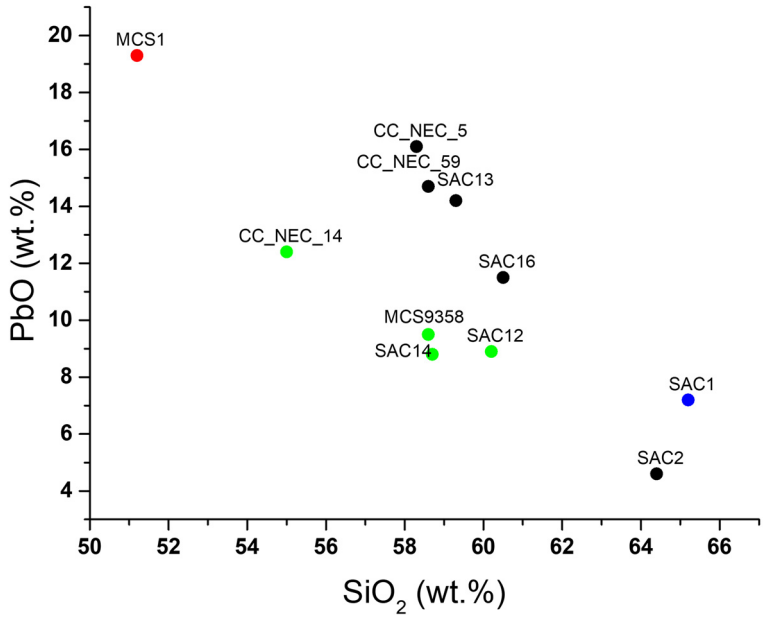

Figure 5. Binary plot of the glaze Pb vs. SiO_2 (wt.%) of the transparent glaze of MJA (dark blue), FLS (black), RFS (green), and G-RFS (red).

Due to the selected analytical method, B_2O_3 could not be detected, although it was certainly present in the glazes. The use of boron in glazes and the reduction in Pb content in

this type of ceramics is well documented [5,9,25]. Additionally, the manuscript (*Pasta nº4, Centro de Documentação Manuel Joaquim Afonso*) kept in the museum's archive describes the addition of borax or boric acid in most glaze recipes (Figure 6). The procedure to prepare glazes is consistent, starting with producing a soda–lime frit, which was then mixed with lead and other components before being milled. Also, Lepierre mentions borax being added to glazes produced by FSL, particularly to the granite ceramic bodies of G-RFS [12,13].

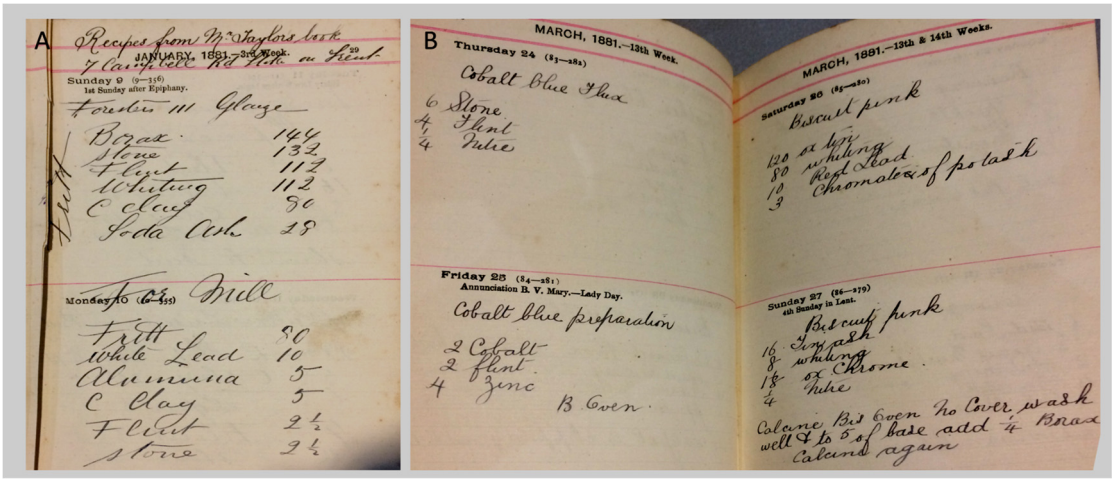

Figure 6. Pages of the manuscript (*Pasta nº4, Centro de Documentação Manuel Joaquim Afonso*) with (**A**) transparent glaze recipe and (**B**) several colours.

All analysed glazes were homogenous regarding their microstructure, with few mineral inclusions. Yet, the interface between the ceramic body and the glaze exhibited a formation of crystals due to interactions between their constituents (Figure 7). Previous studies about white earthenware also reported a broad reaction zone between the glaze and the ceramic body [5]. Larger mineral inclusions were sparsely present in the glazes, like the darker Si-rich rounded particles (Figure 7). These may be remnants of the raw materials that did not dissolve during the firing process or crystals that may have migrated directly from the ceramic body without melting into the glaze. These were identified as quartz by Raman spectroscopy (spectral features at 263, 355, 460, and 505 cm^{-1}) [26]. Smaller elongated crystals seem to have been precipitated during the cooling process. EDS analysis showed that some of these crystals were rich in Al, Si, Na, and Ca (Figure 7b). Raman spectroscopy revealed the characteristic bands of Na-Ca feldspars, with bands at 179, 281, and 408; a strong peak at 508 with two shoulders at 462 and 479 cm^{-1}; and smaller bands at 564, 700, and 788 cm^{-1}. Identifying the exact mineral phase was impossible, although spectral features are close to andesine or labradorite [27]. No specific information about the firing cycles used by FLS during this period exists, but other authors have claimed that the technical literature about white earthenware production mentioned long firing cycles and slow cooling [2]. This fact may have favoured the dissolution and precipitation of new mineral phases in the ceramic–glaze interface. Another typology of inclusions showed high Ca and P concentrations through EDS analysis. These were identified as apatite $Ca_5(PO_4)$ by its characteristic Raman spectral features at 965 and 1018 cm^{-1}(Figure 7d) [28]. None of the studied glaze recipes described in the manuscript mentioned the addition of bone ash. Bone was only mentioned in the preparation of some blue colourants. These crystals appear to be close to colourant particles, which may indicate a connection between these particles and the colourant preparation.

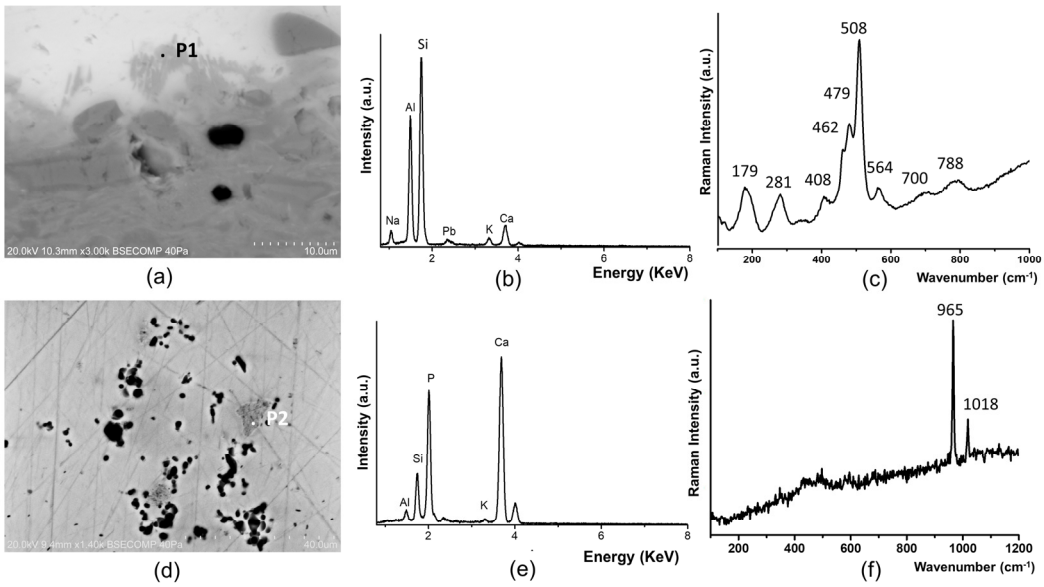

Figure 7. SEM BSE image and spectral features of the inclusions on ceramic SAC12 and glaze SAC1. (**a**) BSE image of the ceramic–glaze interface of sample SAC12; (**b**) EDS-spectra of P1 in image (**a**); (**c**) Raman spectra of Na-Ca Feldspar (SAC12); (**d**) BSE image of sample SAC1; (**e**) EDS-spectra of P2 in image (**d**); and (**f**) Raman spectra of apatite (SAC1).

3.3. Pigments

The early production of FLS mainly involved decoration with monochromatic transfer print motifs (Figure 1) [15,17]. An observation of cross-sections under the optical microscope showed that the colourant was applied under the glaze (Figure 8). All the colours showed little dispersion in the transparent glaze, except for the intense blue in SAC1 (Figure 8b).

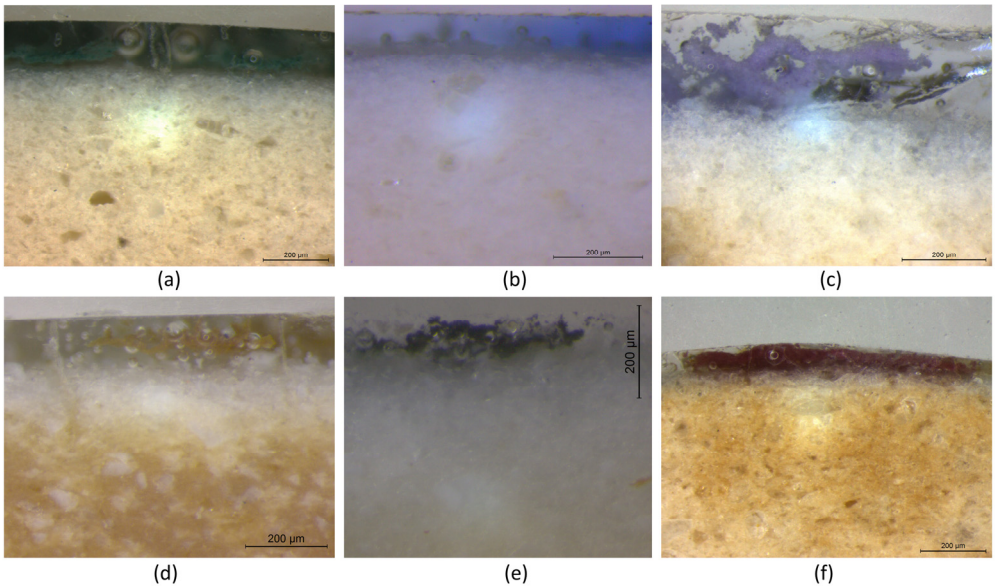

Figure 8. Cross-sections observed under the optical microscope: (**a**) SAC12 Green; (**b**) SAC1 intense blue; (**c**) SAC16 light blue; (**d**) SAC13 brown; (**e**) SAC2 black; and (**f**) MCS9358 pink.

3.3.1. Green

Elemental mapping with VP-SEM showed that the green colour was obtained with a Cr-based pigment. Higher Fe, Zn, and Co concentrations were also detected (Figure 8b), probably added to adjust the tonality of the green. The main mineral phase identified by Raman was Eskolaite (Cr_2O_3) (Figure 9c), with spectral features at 187, 300, 350, 552, 613,

and 693 cm^{-1} [29]. Eskolaite was a green pigment used during the 19th century and a precursor of many pigments produced by the Manufacture de Sèvres [11].

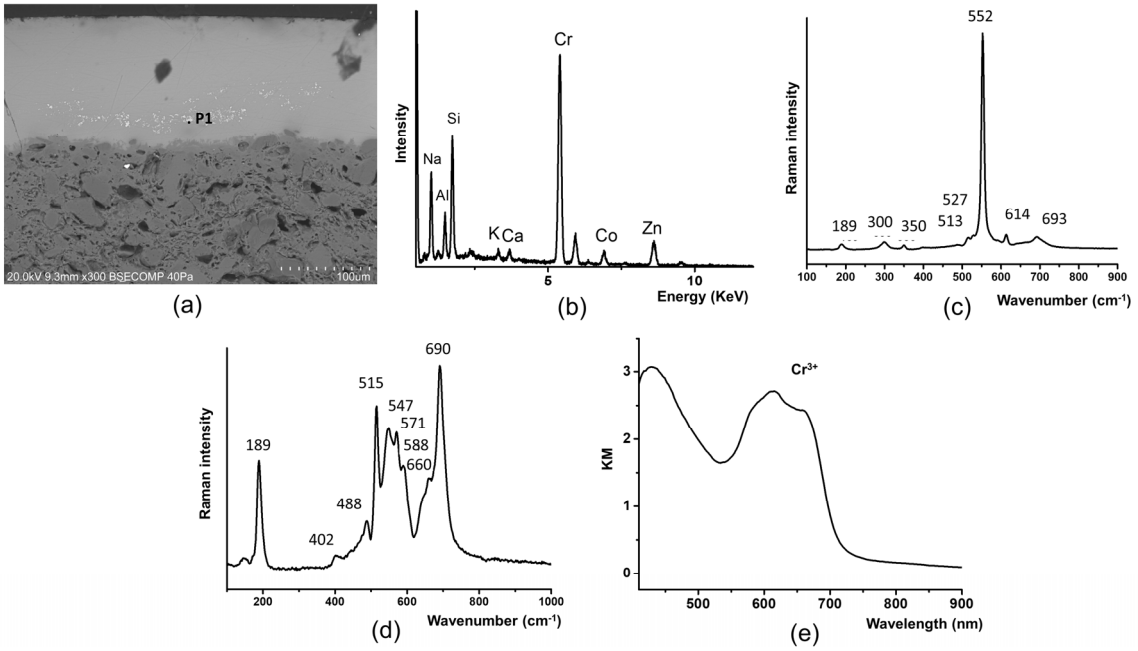

Figure 9. SEM BSE image and spectral feature of the green pigment of sample SAC 12. (**a**) BSE-SEM micrograph; (**b**) EDS spectra of P1 in (**a**) Raman spectra of (**c**) Eskolaite and (**d**) chromite structure; and (**e**) absorption spectral features obtained with Kubelka–Munk processing.

A second mineral phase with bands at 189,402, 488, 515, 547,571,588, and 690 cm^{-1} (Figure 9d) may be attributed to the vibrational modes of a spinel structure. The most intense bands at 189, 515, and 690 could be attributed to F2g(1), F2g(2), and A1g modes. Chemical composition with Cr, Co, and Zn in the spectra could be related to a chromite structure [30]. However, the presence of intermediate phases or mixtures does not allow for the exact identification of the mineral phases. Absorption spectra obtained via HSI (Figure 9e) exhibited the characteristic spectral features of Cr^{3+} ions in octahedral coordination at 640, 600, and 715 nm [31].

Several recipes named "printing green" are described in a manuscript, all with Cr-based compounds, such as chromium oxides or potassium chromate. Zn was also added to green colours in most cases, as observed in the green-painted objects studied (SAC 12 and CC_NEC_14).

3.3.2. Blue

Two types of blue decorations were used in FLS production: (i) a light blue (e.g., SAC16) and (ii) a strong blue (e.g., SAC1 and NEC_CC_61). Both the blue decorations had cobalt as the main colourant, presenting the spectral features of Co^{2+} (Figure 10). Regarding the chemical composition, the light blue colour had cobalt-rich and tin crystals (Figure 10a–c). The Raman spectra showed the main bands at 603, 634, and broadband 716 with a shoulder at 747 cm^{-1} (Figure 10i). Bouchard and Gambardella [32] analysed several groups of cobalt-based spinels and several ortho-stannate solid solutions, $(Co, Mg)_2SnO_4$, and the main bands identified were 775, 668, and 633 cm^{-1}. Chromite structures, such as a cobalt chromite ($CoCr_2O_4$) or a cobalt chromite blue-green ($Co(Al,Cr)_2O_4$) are common blue ceramic pigments [33].

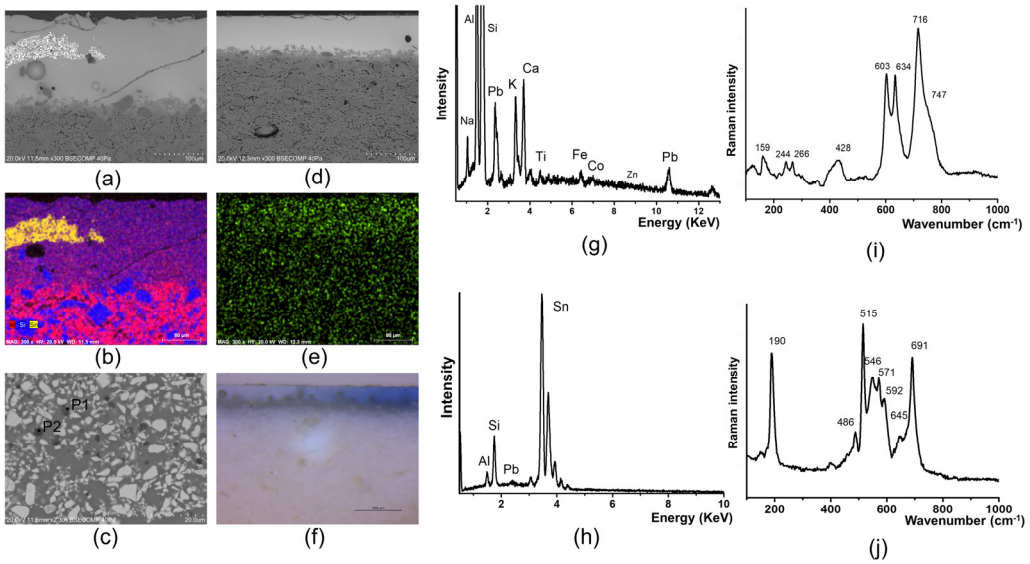

Figure 10. SEM BSE image and spectral features of the glaze and blue pigments of light blue SAC 16 and intense blue CC_NEC_61 samples. (**a**) BSE-SEM micrograph of SAC 16; (**b**) a combination of elemental maps of Al (red), Si (blue), and Sn (yellow) of the image (**a**); (**c**) a higher magnification of the pigment of the image (**a**); (**d**) BSE-SEM micrograph of CC_NEC_61; (**e**) Co map of the image (**d**); (**f**) optical microscope image of CC_NEC_61; (**g**) EDS spectra of P1 in (**c**); and (**h**) EDS spectra of P2 in (**c**); and Raman spectra of (**i**) SAC16 and (**j**) CC_NEC_61.

In the intense blue objects, bands at 190, 515, and 691 cm^{-1} (Figure 10j) are close to $ZnCr_2O_4$ and $ZnCo_2O_4$ [32], similar to the spectral features identified in the green pigment (Figure 8d). The manuscript with glaze and colourant recipes described several blue recipes; the majority are obtained with a cobalt compound, zinc oxide, and alumina. Other blue recipes add zaffre, a cobalt silicate rich in potassium.

3.3.3. Brown

The brown pigment appears to be accumulated in the middle of the glaze and comprises three main elements: Cr, Fe, and Zn (Figure 11a–d). Raman spectra showed two broad bands in the 400–800 cm^{-1} range, with the strongest at ca. 572 cm^{-1} with a lower shoulder at 545 cm^{-1} and another at 689 cm^{-1} with a lower shoulder at 644 cm^{-1} (Figure 11f). The characteristics of the obtained spinel type spectra may be related to the cation disorder [30]. Fe-Cr oxides mixed with Zn or Zn-containing glazes can shift black pigments to brown [34,35].

3.3.4. Black

The black colour is a mixture of several oxides, such as Cr, Co, and Fe (Figure 12a–e). The Raman spectra of particles richer in Cr show a small band at 189 and two broad features, one at ca. 540 cm^{-1} with a shoulder at 582 cm^{-1} and a stronger band at 691 cm^{-1} with a pre-shoulder at 648 cm^{-1} (Figure 12f). The characteristic spectra are close to chromite spectra but slightly shifted to lower frequencies. The characteristic chromite spectra have two strong bands: one at 695 cm^{-1} with a shoulder at 650 cm^{-1} corresponding to mode A1g and another at 566 cm^{-1}. Changes in the Raman spectra have been previously attributed to isomorphic substitution at octahedral sites (Fe^{3+} and Cr^{3+} for Al^{3+}) and disordered chemical substitutions [36]. The position of the A1g band depends on the degree of substitution. Some Sn-rich crystals, which could be used as an opacifier, were also detected (Figure 9). Regarding the Sn-rich particles, the spectra (Figure 12g) seem to combine features related to chromite with cassiterite, which has a major band at 633 cm^{-1} [37], but no isolated spectra of cassiterite was obtained.

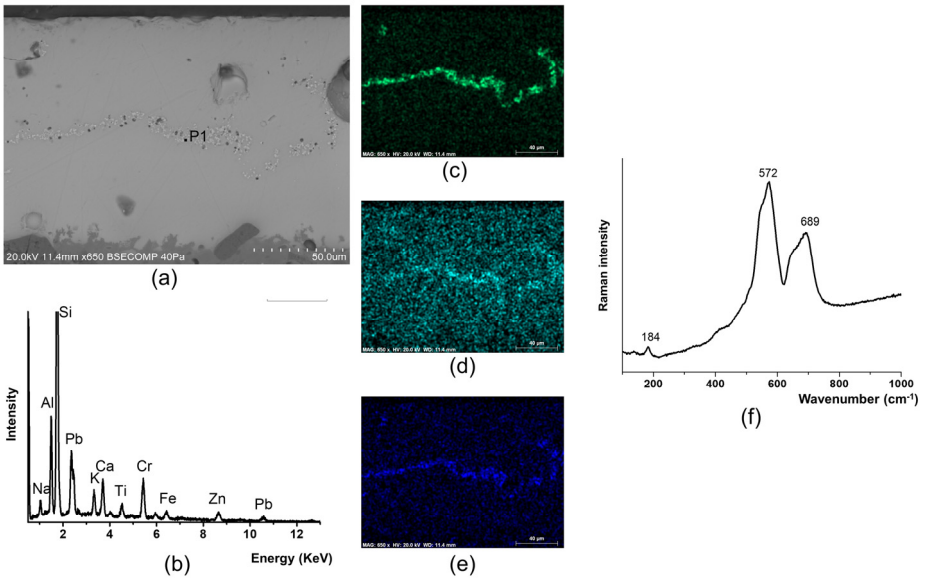

Figure 11. SEM BSE image and spectral features of brown sample SAC 13. (**a**) BSE-SEM micrograph of SAC 13; (**b**) EDS spectra of P1 in image (**a**); Elemental maps of image (**a**) of (**c**) Cr; (**d**) Fe; and (**e**) Zn; (**f**) Raman spectra of Cr, Fe, and Zn spinel structure.

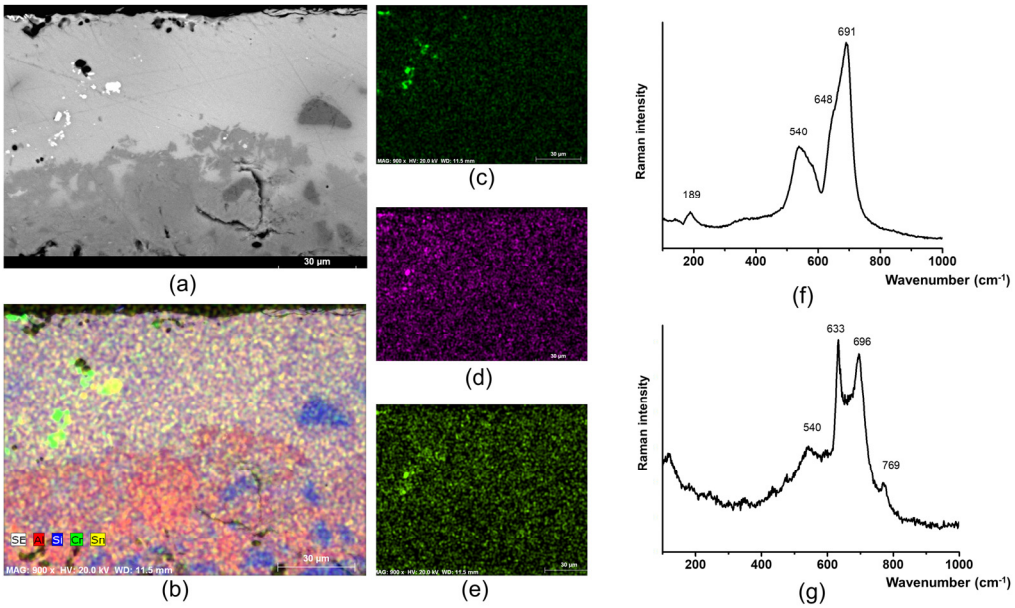

Figure 12. SEM BSE image, elemental maps, and spectral features of the black pigment sample SAC 2. (**a**) BSE-SEM micrograph of SAC 2; (**b**) Combination of SE image (**a**) and elemental map of Al (red), Si (blue), Cr (green), and Sn (yellow); elemental maps of image (**a**) of (**c**) Cr, (**d**) Fe and (**e**) Co; (**f**) Raman spectra of chromium-rich and (**g**) tin-rich particles.

3.3.5. Pink

Tin and a low concentration of Cr represented the elemental composition of the pink areas. The microstructure of the pink pigment showed two types of particles, one Sn-rich and the other Sn-poor (Figure 13a,b). Several HSI results showed a strong absorption band at 520 nm (Figure 13c), which can be assigned to Cr^{4+} in an octahedral site, according to the literature on chromium-doped tin pigments [38]. The particles richer in Sn were identified by Raman as chromium-doped malayaite with a strong band at 740 cm^{-1} and weaker at 940 cm^{-1} (Figure 13d,e). This chromophore has been previously identified in different glazed and glass objects with bands at ca. 761–775 cm^{-1} and 942–963 cm^{-1} in the literature

on chromium-doped tin pigments [39,40]. Chromium-doped tin sphene is a pink pigment that remains stable at 1280 °C or above. The chemistry is complex; basically, a pink pigment is obtained from a mixture of calcite ($CaCO_3$), tin oxide (SnO_2), silica (SiO_2), and potassium chromate ($K_2Cr_2O_7$).

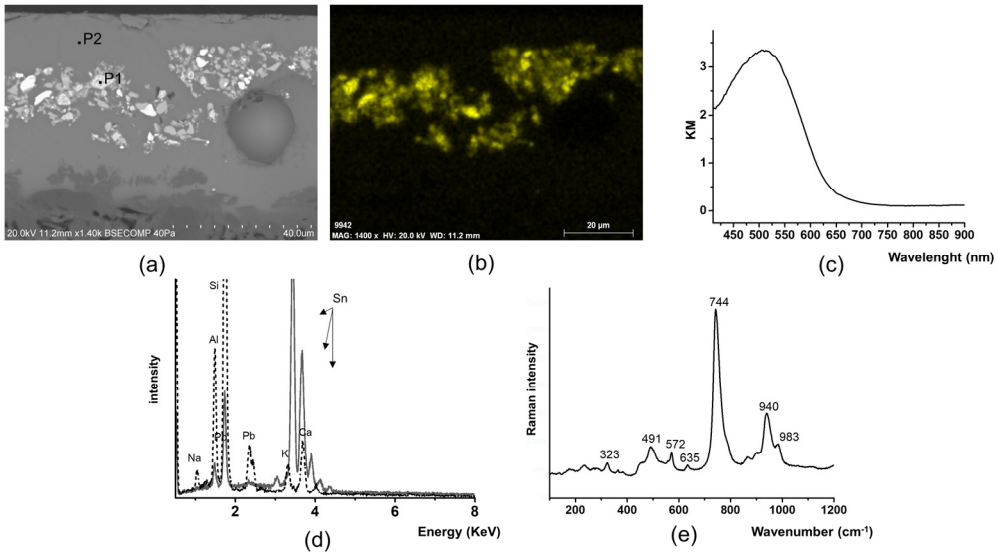

Figure 13. SEM BSE and spectral features of the pink sample MCS9358. (**a**) BSE-SEM micrograph; (**b**) Sn elemental map of image (**a**); (**c**) absorption spectral features obtained with Kubelka–Munk processing; (**d**) EDS spectra of P1 (full grey) and P2 (dot) in image (**a**); (**e**) Raman spectra of malayaite.

In summary, the results showed that the type of ceramic used in FLS during the first 50 years of production was a Ca-poor white earthenware type. The glazing technology consisted of applying a transparent glaze over the ceramic body, which is different from the traditional Portuguese tin-glazed ceramics [41,42]. The colourants were applied under the glaze, and these also denote technological advancements compared to the colour palette of Portuguese ceramic production in earlier periods [16], particularly the chromium-based pigments.

4. Conclusions

Through a multianalytical approach, this work provides the first material characterisation of the tableware produced by the FLS ceramic manufactory. The results provide a generic overview of the materials and technological methods used by this manufactory during the first 50 years of production. During this period, the ceramic body was composed of a Si-Al matrix with high-temperature crystalline phases, such as mullite and cristobalite, and also had a considerable amount of quartz inclusions. Although the type of ceramic was maintained during this period, some variations in the recipes and type of raw materials (type of Si-rich particles and glassy phase former) could be detected requiring further investigation. The glaze applied over the ceramic body was a transparent lead-alkali glaze. Differences regarding the Si, Ca, and Pb ratio may be related to the substitution of Pb by B (not analysed in this study). Except for the deep blue colour obtained with cobalt dispersed in the glaze, all other colours (light blue, green, brown, black, and pink) did not disperse in the glassy phase. Many colours were obtained with Cr-based compounds accompanying the modern pigments used in European ceramic manufactories during this period.

Supplementary Materials: The following supporting information can be downloaded at https://www.mdpi.com/article/10.3390/min14030324/s1, Table S1: Composition (max.–min.) in oxides (wt.%) of the ceramic body (n = 1) measured by EDS analysis.

Author Contributions: Conceptualization, M.L.C., J.P.V. and A.R.; methodology, M.L.C., J.P.V., A.R., L.D., M.M.R.A.L. and S.B.-S.; validation, M.L.C., J.P.V., T.P.d.S., A.R., P.V. and S.B.-S.; formal analysis, M.L.C., J.P.V., A.R., P.V. and S.B.-S.; investigation, M.L.C., J.P.V., A.R., C.P., A.R., A.C.D. and J.C.R.; resources, M.L.C., J.P.V., A.R., C.P., A.R., A.C.D. and J.C.R.; data curation, M.L.C., J.P.V. and A.R.; archival and documental research, C.P. and A.C.D. writing—original draft preparation, M.L.C., J.P.V., A.R., M.M.R.A.L., C.P., A.R., A.C.D. and J.C.R. All authors have read and agreed to the published version of the manuscript.

Funding: This work was supported by National Funds through the Portuguese Foundation for Science and Technology (FCT-MCTES) under the projects UID-B/50025/2020 i3N/CENIMAT FCT-UNL; 10.54499/UIDB/00729/2020 and 10.54499/UIDP/00729/2020 VICARTE/ FCT-UNL; and UIDB/04449/2020 and UIDP/04449/2020 HERCULES/UE; LA/P/0132/2020 (Laboratório Associado IN2PAST); the contract 10.54499/CEECIND/00349/2017/CP1431/CT0004 (M. L. Coutinho) and 10.54499/2020.00252.CEECIND/CP1586/CT0002 (A. Ruivo); CityUMacau Chair in Sustainable Heritage.

Data Availability Statement: Data are contained within the article and Supplementary Materials.

Acknowledgments: The authors would like to thank Câmara Municipal de Loures, [9]Associação dos Amigos da Loiça de Sacavém, and Instituto de Gestão do Património Arquitectónico e Arqueológico. The authors would like to acknowledge the reviewers of the manuscript.

Conflicts of Interest: The authors declare no conflicts of interest.

References

1. Maggetti, M.; Rosen, J.; Serneels, V. The origin of 18th–19th century tin-glazed pottery from Lorraine, France. *Archaeometry* **2015**, *57*, 426–452. [CrossRef]
2. Maggetti, M.; Serneels, V.; Stasch, G. Journal of Archaeological Science: Reports Composition and technology of 18th century high magnesia faïences from Fulda. *J. Archaeol. Sci. Rep.* **2015**, *2*, 40–50. [CrossRef]
3. Maggetti, M. Archaeometric Analyses of European 18th–20th Century White Earthenware—A Review. *Minerals* **2018**, *8*, 269. [CrossRef]
4. Beauvoit, E.; Ben Amara, A.; Cantin, N.; Lemasson, Q.; Sireix, C.; Marache, V.; Chapoulie, R. Technological investigation on ceramic bodies of 19th century French white earthenware from the Bordeaux region. *J. Archaeol. Sci. Rep.* **2020**, *31*, 102314. [CrossRef]
5. Maggetti, M.; Heege, A.; Serneels, V. Technological aspects of an early 19th c. English and French white earthenware assemblage from Bern (Switzerland). *Period. Mineral.* **2015**, *84*, 139–168. [CrossRef]
6. Kováč, J.; Trník, A.; Medved', I.; Vozár, L. Influence of calcite in a ceramic body on its thermophysical properties. *J. Therm. Anal. Calorim.* **2013**, *114*, 963–970. [CrossRef]
7. Emiliani, G.P.; Corbara, F. *Tecnologia Ceramica—Le Materie Prime*; Grupo Editoriale Faenza Editrice S.p.A.: Faenza, Italy, 1999; ISBN 88-8138-043-9.
8. Maggetti, M.; Rosen, J.; Serneels, V. White earthenware from Loraine (1755–*c*. 1820): Provenance and technique. *Archaeometry* **2011**, *4*, 765–790. [CrossRef]
9. Beauvoit, E.; Ben Amara, A.; Tessier-Doyen, N.; Frugier, C.; Lemasson, Q.; Moignard, B.; Pacheco, C.; Pichon, L.; Chapoulie, R.; Gratuze, B. Chemical and Mechanical Characterisation of White Earthenware Glazes from the Johnston-Vieillard Manufactory (France, 19th Century). *Archaeometry* **2021**, *63*, 941–959. [CrossRef]
10. Samford, P.M. Response to a market: Dating english underglaze transfer-printed wares. *Hist. Archaeol.* **1997**, *31*, 1–30. [CrossRef]
11. Verger, L.; Dargaud, O.; Chassé, M.; Trcera, N.; Rousse, G.; Cormier, L. Synthesis, properties and uses of chromium-based pigments from the Manufacture de Sèvres. *J. Cult. Herit.* **2018**, *30*, 26–33. [CrossRef]
12. Lepierre, C. *Estudo Chimico e Technologico Sobre a Cerâmica Portugueza Moderna*; Imprensa Nacional: Lisboa, Portugal, 1899.
13. Lepierre, C. *Estudo Chimico e Technologico Sobre a Cerâmica Portuguesa Moderna*, 2nd ed.; do Fomento, M., Ed.; Tipografia da Associação de Classe fos Compositores Tipográficos: Lisbon, Portugal, 1912.
14. Queirós, J. *A Cerâmica Portuguesa e Outros Estudos*, 3rd ed.; Editorial Presença, Lda: Lisboa, Portugal, 1987.
15. Varios. *Sacavém, a Outra Loiça*; Camara Municipal de Loures: Loures, Portugal, 2019; ISBN 978-972-914-9142-58-1.
16. Figueiredo, E.; Esteves, L.; Pais, A.N.; Vilarigues, M.G.; Coentro, S.X. As cores na azulejaria portuguesa: Uma revisão. *Conserv. Património* **2023**, *42*, 72–80. [CrossRef]
17. Assunção, A.P. *150 Anos—150 Peças Fábrica de Loiça de Sacavém*; Museu de Cerâmica de Sacavém, Mirandela-Artes Gráficas, S.A.: Loures, Portugal, 2006; ISBN 972-9142-33-5.
18. Assunção, A.P.; Pereira, C.; Correia, E. *Primeiras Peças da Produção da Fábrica de Loiça de Sacavém—O Papel do Coleccionador*; António Coelho Dias, Museu de Cerâmica de Sacavém: Loures, Portugal, 2003.
19. Pereira, C.; Pina, J.; Rodrigues, G.; David, F. *Intenerário pela Produção da Fábrica de Loiça de Sacavém—Museu de Cerâmica de Sacavém*; Palmigráfica, Artes Gráficas: Loures, Portugal, 2000.

20. Aras, A. The change of phase composition in kaolinite- and illite-rich clay-based ceramic bodies. *Appl. Clay Sci.* **2004**, *24*, 257–269. [CrossRef]
21. Lee, S.; Kim, Y.J.; Moon, H.S. Phase transformation sequence from kaolinite to mullite investigated by an energy-filtering transmission electron microscope. *J. Am. Ceram. Soc.* **1999**, *82*, 2841–2848. [CrossRef]
22. Pressler, E.E.; Shearer, W.L. *Properties of Potters' Flints and Their Effects in White-Ware Bodies*; Department of Commerce Bureau of Standards: Governmen Printing Office: Washington, DC, USA, 1926; Volume 20.
23. Weymouth, J.H.; Williamson, W.O. Some physical properties of raw and calcined flint. *Mineral. Mag. J. Mineral. Soc.* **1951**, *29*, 573–593. [CrossRef]
24. Chargui, F.; Hamidouche, M.; Belhouchet, H.; Jorand, Y.; Doufnoune, R.; Fantozzi, G. Mullite fabrication from natural kaolin and aluminium slag. *Bol. Soc. Esp. Ceram. Vidr.* **2018**, *57*, 169–177. [CrossRef]
25. Bouquillon, A.; Castaing, J.; Barbe, F.; Crepin-Leblond, T.; Tilliard, L.; Paine, S.R.; Christman, B.; Heuer, A.H. French Decorative Ceramics Mass-Produced during and After the 17th Century: Chemical Analyses of the Glazes. *Archaeometry* **2018**, *60*, 946–965. [CrossRef]
26. Coentro, S.; Mimoso, J.M.; Lima, A.M.; Silva, A.S.; Pais, A.N.; Muralha, V.S.F. Multi-analytical identification of pigments and pigment mixtures used in 17th century Portuguese azulejos. *J. Eur. Ceram. Soc.* **2012**, *32*, 37–48. [CrossRef]
27. Freeman, J.J.; Wang, A.; Kuebler, K.E.; Jolliff, B.L.; Haskin, L.A. Characterization of natural feldspars by raman spectroscopy for future planetary exploration. *Can. Mineral.* **2008**, *46*, 1477–1500. [CrossRef]
28. Rogers, K.D.; Daniels, P. An X-ray diffraction study of the effects of heat treatment on bone mineral microstructure. *Biomaterials* **2002**, *23*, 2577–2585. [CrossRef]
29. Bouchard, M.; Smith, D.C.D.C.; Carabatos-Nédelec, C. An investigation of the feasibility of applying Raman microscopy for exploring stained glass. *Spectrochim. Acta A Mol. Biomol. Spectrosc.* **2007**, *68*, 1101–1113. [CrossRef]
30. D'Ippolito, V.; Andreozzi, G.B.; Bersani, D.; Lottici, P.P. Raman fingerprint of chromate, aluminate and ferrite spinels. *J. Raman Spectrosc.* **2015**, *46*, 1255–1264. [CrossRef]
31. Liang, S. Colour performance investigation of a Cr_2O_3 green pigment prepared via the thermal decomposition of CrOOH. *Ceram. Int.* **2014**, *40*, 4367–4373. [CrossRef]
32. Bouchard, M.; Gambardella, A. Raman microscopy study of synthetic cobalt blue spinels used in the field of art. *J. Raman Spectrosc.* **2010**, *41*, 1477–1485. [CrossRef]
33. Forés, A.; Llusar, M.; Badenes, J.A.; Calbo, J.; Tena, M.A.; Monrós, G. Cobalt minimisation in willemite (Co_xZn_2-$xSiO_4$) ceramic pigments. *Green Chem.* **2000**, *2*, 93–100. [CrossRef]
34. Caggiani, M.C.; Colomban, P. Raman identification of strongly absorbing phases: The ceramic black pigments. *J. Raman Spectrosc.* **2011**, *42*, 839–843. [CrossRef]
35. Yurdakul, H.; Turan, S.; Ozel, E. The mechanism for the colour change of iron chromium black pigments in glazes through transmission electron microscopy techniques. *Dye. Pigment.* **2011**, *91*, 126–133. [CrossRef]
36. Dondi, M.; Zanelli, C.; Ardit, M.; Cruciani, G.; Mantovani, L.; Tribaudino, M.; Andreozzi, G.B. Ni-free, black ceramic pigments based on Co–Cr–Fe–Mn spinels: A reappraisal of crystal structure, colour and technological behaviour. *Ceram. Int.* **2013**, *39*, 9533–9547. [CrossRef]
37. Coentro, S.; Da Silva, R.C.; Relvas, C.; Ferreira, T.; Mirão, J.; Pleguezuelo, A.; Trindade, R.; Muralha, V.S.F. Mineralogical Characterization of Hispano-Moresque Glazes: A μ-Raman and Scanning Electron Microscopy with X-ray Energy Dispersive Spectrometry (SEM-EDS) Study. *Microsc. Microanal.* **2018**, *24*, 300–309. [CrossRef]
38. Lopez-Navarrete, E.; Caballero, A.; Orera, V.M.; Lázaro, F.J.; Ocaña, M. Oxidation state and localization of chromium ions in Cr-doped cassiterite and Cr-doped malayaite. *Acta Mater.* **2003**, *51*, 2371–2381. [CrossRef]
39. Faurel, X.; Vanderperre, A.; Colomban, P. Pink pigment optimization by resonance Raman spectroscopy. *J. Raman Spectrosc.* **2003**, *34*, 290–294. [CrossRef]
40. Fischbach, N.; Ngo, A.T.; Colomban, P.; Pauly, M. Beads excavated from Antsiraka Boira Necropolis (Mayotte Island, 12th–13th centuries) colouring agents and glass matrix composition comparison with contemporary Southern Africa sites. *ArcheoSciences* **2016**, *40*, 83–102. [CrossRef]
41. Vieira Ferreira, L.F.; Gonzalez, A.; Pereira, M.F.C.; Santos, L.F.; Casimiro, T.M.; Ferreira, D.P.; Conceição, D.S.; Machado, I.F. Spectroscopy of 16th century Portuguese tin-glazed earthenware produced in the region of Lisbon. *Ceram. Int.* **2015**, *41*, 13433–13446. [CrossRef]
42. Buzanich, A.C. Spectroscopic Techniques for Characterizing Portuguese Glazed Ceramics: A Contributin to the Study of Ancient Faiences of Coimbra. Ph.D. Thesis, Universidade de Lisboa, Faculdade de Ciências, Lisboa, Portugal, 2013.